RAPID COMMUNICATIONS

PHYSICAL REVIEW B VOLUME 35, NUMBER 10 1 APRIL 1987

Diatomic melting curves to very high pressure

D. A. Young
Lawrence Livermore National Laboratory, University of California, Livermore, California 94550

C.-S. Zha,* R. Boehler,† J. Yen, and M. Nicol
Department of Chemistry and Biochemistry, University of California, Los Angeles, California 90024

A. S. Zinn‡
University of California, Los Angeles, California 90024
and Los Alamos National Laboratory, University of California, Los Alamos, New Mexico 87545

D. Schiferl and S. Kinkead
Los Alamos National Laboratory, University of California, Los Alamos, New Mexico 87545

R. C. Hanson and D. A. Pinnick
Department of Physics, Arizona State University, Tempe, Arizona 85287
(Received 15 October 1986)

Using new high-temperature diamond-anvil-cell designs, together with a variety of optical techniques, we have measured the melting curves of N_2 to 18.0 GPa, O_2 to 16.3 GPa, and F_2 to 2.5 GPa. One triple point is found on the N_2 curve and two on the O_2 curve. A simple "effective rotation" model of librational motions in the solid is used to obtain good theoretical fits to the experimental curves.

Recent improvements in the design of externally heated diamond-anvil cells (DAC's) allow direct observations and spectroscopic investigations of material under high pressure and at temperatures of 1000 K and higher. These developments greatly increase the range over which melting curves of low-melting-temperature molecular solids can be determined.

The homonuclear diatomic solids are especially interesting for melting studies because of their low melting temperatures and complex phase diagrams.[1-5] For N_2, O_2, and F_2, previous work followed the melting curves to 2.8, 7.0, and 0.01 GPa, respectively.[6-8] In this Rapid Communication, we report the extension of these melting curves to much higher pressures and temperatures. In addition, we consider a simple theoretical model for melting in diatomic solids.

The melting curves were determined with DAC's externally heated with resistance heaters to provide uniform temperatures and pressures. Temperatures were determined with thermocouples placed at several spots on the cell. For temperatures below 700 K, pressures were determined by the ruby-fluorescence method.[9] For N_2 above 700 K, the pressure was determined from the vibron frequency.[10]

The DAC's used were of the Hirsch-Holzapfel,[11] Merrill-Bassett,[12] and Boehler[13] designs. For temperatures up to the range 600–700 K, the usual materials used to construct the cells are adequate. However, above 700 K, the load-bearing materials are subject to rapid creep deformation, the diamonds oxidize in air, and the gaskets either weld to the diamond anvils or react with the N_2 or O_2 samples.

In order to extend the temperature range, we constructed a special DAC based on the Merrill-Bassett design, using the most temperature-resistant materials. The cell was operated in a vacuum oven to prevent oxidation of the diamond anvils. Uniform temperatures around the sample were obtained by placing the entire DAC in a container.

No perfectly satisfactory gaskets were found. Inconel 718 gaskets did not react with N_2, O_2, or F_2, but they did weld to the diamonds above about 550 K and 5 GPa. Opening the cell afterwards always caused the diamonds to fracture. Re and Mo–13 wt.% Re gaskets were tried as alternatives, but these materials reacted with the O_2 and N_2 samples.

N_2 samples were loaded by the immersion,[14] indium dam,[15] or high-pressure gas[15] techniques, with the last used for most of the measurements above 600 K. We used a number of techniques, including Raman spectroscopy, interferometry, light scattering, and direct visual observation, to detect melting. By far the most reliable technique was Raman spectroscopy because the vibron peaks in the β, δ, and fluid phases N_2 differ markedly from each other. The upper limit on the interferometry was about 9 GPa because of imperfections in the sample and misalignment of the diamond culets. Visual observations also became difficult above 9 GPa, but could still be used up to about 11 GPa. The melting temperatures determined by light scattering were considerably lower than those determined by Raman spectroscopy or visual observations. Presumably, the scattering from the grain boundaries was reduced as the samples annealed to form single crystals well below the actual melting temperature.

Up to about 700 K, pressures were determined with the ruby-fluorescence method. Above this temperature, the N_2 vibron-pressure scale was used. Zinn, Schiferl, and

Nicol[10] have shown that the vibron frequencies ν_2 of δ-N_2 and ν_{fluid} in the fluid have the same pressure dependence and a negligible temperature dependence over the range of interest for this work. The pressures in GPa were determined from the N_2 vibron frequencies in cm^{-1} according to the following equation:

$$P = 0.4242\nu - 987.8 \ . \tag{1}$$

Equation (1), which is independent of temperature, was determined by comparing N_2 vibron frequencies at temperatures up to 740 K with pressures determined by the ruby-fluorescence scale. Equation (1) represents the best linear fit of the N_2 vibron frequencies in the high-density δ and fluid phases, extrapolating to $\nu_2(0) = \nu_{\text{fluid}}(0) = 2328.6$ cm^{-1}, in reasonable agreement with the measured $P=0$ gas-phase value[16] of $\nu(0) = 2330.87$ cm^{-1}.

O_2 samples were loaded with the indium dam method. Melting was observed visually and at lower temperatures by changes in the position of the O_2 vibron peak. Near the β-ϵ-fluid triple point, visual observation is particularly effective because the three phases are dramatically different in appearance. The fluid is clear and colorless, the β phase is yellow, and the ϵ phase is either rust-red or orange, depending on the orientation of the crystallites. The melting curve of O_2 was determined only just past the β-ϵ-fluid triple point at 16.3 GPa. The absence of an O_2 vibron-pressure scale analogous to that of N_2, and the fact that much higher pressures are required at high temperatures for O_2, make it difficult to extend the O_2 melting curve further.

F_2 is a difficult and dangerous substance to study in a DAC. After about ten attempts, one F_2 sample was loaded in a special hood with the indium dam method. Further attempts to load more samples were halted after the liquid F_2 in the indium dam exploded. At high pressure, the sample slowly degraded because the F_2 reacted with the diamond anvils to form CF_4, which in turn underwent photochemical reactions to form brown particles of unknown composition. Melting was observed visually and by Raman spectroscopy. The diamonds broke before the melting curve could be fully determined. Experimental difficulties limited the accuracy of the F_2 melting curve. At the highest pressure of 2.5 GPa, the uncertainty in temperature is ± 23 K.

Details of the DAC designs, experimental procedures, and melting curve data will be published elsewhere. The smoothed experimental melting curves of N_2, O_2, and F_2 are tabulated in Table I and are compared to that of H_2 (Ref. 17) in Fig. 1. The melting curves of N_2 and F_2 are very close together, but the O_2 curve is very different and is so steep that it crosses the H_2 curve near room temperature.

There are no triple points on the melting curve of F_2 up to 320 K; however, the melting curves of N_2 and O_2 are complicated by changes in curvature around these points. In N_2, we find one triple point (β-δ-fluid) at 580 ± 10 K and 9.9 ± 0.5 GPa. O_2 has two triple points at 283 ± 4 K and 5.0 ± 0.3 GPa (β-γ-fluid) and at 645 ± 10 K and 16.3 ± 0.7 GPa (β-ϵ-fluid).

In order to calculate the melting curves of the three diatomic solids, we begin by assuming a spherically symmetric intermolecular potential. Such simple potentials have been found useful in fitting diatomic fluid equations of state.[18,19] We use the following convenient exponential-6 potential:

$$\phi(r) = \varepsilon\left\{\frac{6}{\alpha-6}\exp\left[\alpha\left(1-\frac{r}{r_m}\right)\right] - \frac{\alpha}{\alpha-6}\left(\frac{r_m}{r}\right)^6\right\} . \tag{2}$$

Here the potential parameters have been obtained by assuming corresponding states[18] with Ar (α) and by fitting

TABLE I. Smoothed experimental melting curves of N_2, O_2, and F_2.

P (GPa)	N_2 T (K)	O_2 T (K)	F_2 T (K)
0	63.2	54.4	53.6
0.5	141	104	136
1.0	194	137	189
1.5	237	163	234
2.0	271	185	271
2.5	300	206	308
3.0	323	223	...
4.0	368	253	...
5.0	410	283	...
6.0	448	317	...
7.0	484	352	...
8.0	518	386	...
9.0	551	419	...
10.0	585	453	...
11.0	626	485	...
12.0	666	517	...
13.0	705	548	...
14.0	745	579	...
15.0	783	609	...
16.0	822	638	...
17.0	861	...	...
18.0	897	...	...

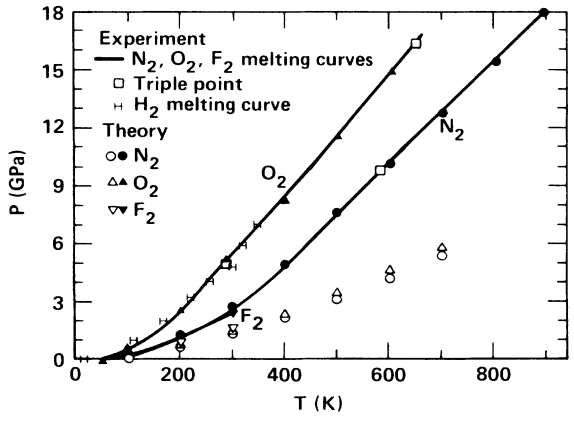

FIG. 1. Comparison of experimental N_2, O_2, and F_2 melting curves with theory based on (1) only monatomic intermolecular potentials (open symbols), and (2) monatomic potentials plus rotational free energy terms (filled symbols). The experimental H_2 melting curve is also shown for comparison.

to fluid equation-of-state[20] data (ε and r_m). For N_2, $\alpha=13.0$, $r_m=4.10$ Å, and $\varepsilon/k=102$ K; for O_2, $\alpha=13.0$, $r_m=3.84$ Å, and $\varepsilon/k=125$ K; and for F_2, $\alpha=13.0$, $r_m=3.68$ Å, and $\varepsilon/k=116$ K. For the solid we assume an fcc lattice and calculate the free energy using quasiharmonic lattice dynamics plus an anharmonic correction, and for the liquid we use a modified hard-sphere perturbation theory with quantum correction.[21] The calculated melting curves are compared with experiment in Fig. 1. It is clear that the theoretical melting pressures are much too low.

The discrepancy is mainly due to the neglect of molecular rotation. If the rotational motions of the molecules in the solid and liquid were the same, the rotational contribution to the free energy would cancel out and have no effect on the calculation of the melting curve, as is true for H_2.[22] However, the rotational motions in solid and liquid are not the same, and the substantial difference between the solid and liquid rotational free energies strongly influences the melting curve. We therefore recalculate the melting curve using very simple models of molecular rotation in the solid and liquid.

For the liquid we assume that the thermally averaged rotational motion is that of a free rotator. The free energy of free rotation in the classical limit is $A/NkT = -\ln(T/2\Theta_r)$, where the factor of 2 arises from the symmetry of the homonuclear molecule, $\Theta_r=h^2/(8\pi^2 Ik)$, and I is the moment of inertia. For the solid we approximate the librational motions as perturbed rotation with an "effective" rotational temperature Θ_s. Because the rotation in the solid will depend on the strength of the intermolecular repulsions, Θ_s will have a volume dependence which we assume to be given by a simple Grüneisen prescription: $\Theta_s=\Theta_0\exp(\gamma_0 x)$, where $x=(V_0-V)/V_0$. In this recalculation of the melting curves, the volume-dependent rotational free energy is added to the previously computed solid free energy and a free-rotator free energy is added to the liquid free energy. The two parameters Θ_0 and γ_0 are then adjusted to give an optimum fit to the experimental melting curve.

The results of the fitting are shown in Fig. 1. The fits are satisfactory, which shows that the librational motion in the solid can be represented by an effective rotation.

We can check the fitted Θ_s parameters against realistic estimates of the energy barriers that perturb rotation in the solid phase. This is best done for N_2, for which the angle-dependent intermolecular potential has been extensively studied.[23,24] The first step is to relate $\Theta_s(V)$ to an effective rotational energy barrier. This can be done approximately with quantum-mechanical perturbation theory. For simplicity, we assume that the perturbation is a δ function, $A\delta(\cos\theta)$. The δ function gives the perturbation term a very simple form which can be calculated readily. The resulting perturbed energies are then summed up into a partition function which is fitted to the value $q=(T/2\Theta_s)$ in order to obtain the energy barrier A.

The second step is to compute the rotational barrier from an optimized atom-atom potential for N_2.[24] A molecule surrounded by 12 nearest neighbors is rotated through $0\leq\theta\leq 180°$, and the energy barrier is taken as the difference between the maximum and minimum potential energies. These two energy curves are shown in Fig. 2. The agreement between them shows that the perturbed rotator model is a reasonable explanation of the N_2 melting curve.

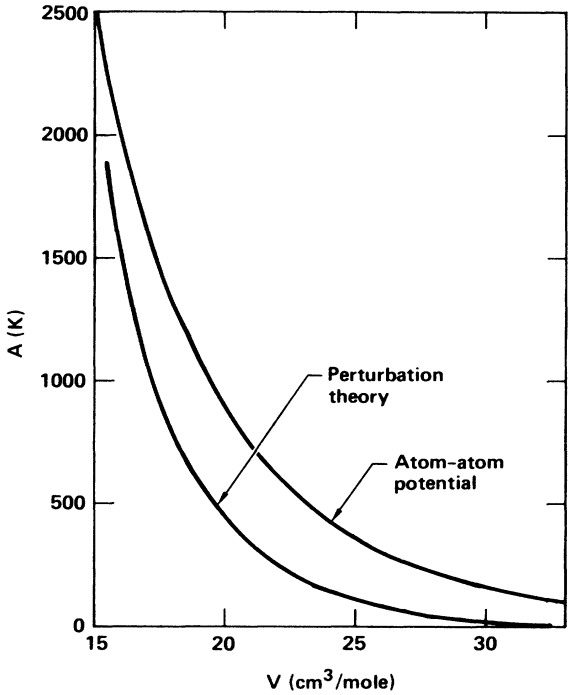

FIG. 2. Rotational energy barrier for solid N_2 computed from quantum perturbation theory fitted to experiment and from an atom-atom potential, as a function of volume.

The anomalous O_2 melting curve may be due to the triplet electronic configuration in O_2, which allows π-electron bonding between molecules. An indication of this bonding is the unusual color of high-pressure O_2. At 11 GPa it is reddish, and it becomes black by 40 GPa.[25] Intermolecular bonding in the solid would more effectively inhibit free rotation and thereby increase the melting pressure, as observed.

There remains the difficult theoretical problem of calculating the melting curves of diatomic solids from accurate angle-dependent potentials. Molecular dynamics simulations[26,27] have been successful in elucidating the rotational states of the molecules in the compressed solid phases of N_2 and O_2, and it may be that such simulations applied to the computation of diatomic melting curves will also be successful.

This work was performed under the auspices of the U. S. Department of Energy by Lawrence Livermore National Laboratory under Contract No. W-7405-ENG-48, and by Los Alamos National Laboratory under Contract No. W-7405-ENG-36. R.B., M.N., and C.-S.Z. acknowledge partial support from NSF Grant No. EAR-8507755, and Department of Energy Grant No. DE-AT03-81ER10965. M.N., J.Y., and A.S.Z. acknowledge support from NSF Grant No. DMR 83-18812. We thank D. Kli-

ner for assistance with the O_2 experiments. We are also pleased to acknowledge grants from the Livermore and Los Alamos branches of the University of California Institute of Geophysics and Planetary Physics. The work of R.C.H. and D.A.P. was performed while they were at Los Alamos National Laboratory.

---

*Present address: Geophysical Laboratory, Carnegie Institution of Washington, Washington, DC 20008.

†Present address: Max-Planck-Institut für Chemie, Saarstrasse 23, D-6500 Mainz, West Germany.

‡Present address: Department of Chemistry, University of California, Berkeley, CA 94720.

[1]R. L. Mills, B. Olinger, and D. T. Cromer, J. Chem. Phys. **84**, 2837 (1986).

[2]S. Buchsbaum, R. L. Mills, and D. Schiferl, J. Phys. Chem. **88**, 2522 (1984).

[3]D. Schiferl, S. Buchsbaum, and R. L. Mills, J. Phys. Chem. **89**, 2324 (1985).

[4]R. Reichlin, D. Schiferl, S. Martin, C. Vanderborgh, and R. L. Mills, Phys. Rev. Lett. **55**, 1464 (1985).

[5]B. Olinger, R. L. Mills, and R. B. Roof, Jr., J. Chem. Phys. **81**, 5068 (1984).

[6]J. D. Grace and G. C. Kennedy, J. Phys. Chem. Solids **28**, 977 (1967).

[7]H. d'Amour, W. B. Holzapfel, and M. Nicol, J. Phys. Chem. **85**, 130 (1981).

[8]G. C. Straty and R. Prydz, Phys. Lett. **31A**, 301 (1970).

[9]J. D. Barnett, S. Block, and G. J. Piermarini, Rev. Sci. Instrum. **44**, 1 (1973).

[10]A. S. Zinn, D. Schiferl, and M. Nicol (unpublished).

[11]K. R. Hirsch and W. B. Holzapfel, Rev. Sci. Instrum. **52**, 52 (1981).

[12]L. Merrill and W. A. Bassett, Rev. Sci. Instrum. **45**, 290 (1974).

[13]R. Boehler (unpublished).

[14]D. Schiferl, D. T. Cromer, and R. L. Mills, High Temp. High Pressures **10**, 493 (1978).

[15]R. L. Mills, D. H. Liebenberg, J. C. Bronson, and L. C. Schmidt, Rev. Sci. Instrum. **51**, 891 (1980).

[16]G. Herzberg, *Spectra of Diatomic Molecules* (Van Nostrand, Toronto, 1950), p. 62.

[17]V. Diatschenko *et al.*, Phys. Rev. B **32**, 381 (1985).

[18]M. Ross and F. H. Ree, J. Chem. Phys. **73**, 6146 (1980).

[19]D. MacGowan *et al.*, J. Chem. Phys. **80**, 2719 (1984).

[20]N. B. Vargaftik, *Tables on the Thermophysical Properties of Liquids and Gases* (Wiley, New York, 1975).

[21]D. A. Young, A. K. McMahan, and M. Ross, Phys. Rev. B **24**, 5119 (1981).

[22]D. A. Young and M. Ross, J. Chem. Phys. **74**, 6590 (1981).

[23]F. H. Ree and N. W. Winter, J. Chem. Phys. **73**, 322 (1980).

[24]J. D. Johnson, M. S. Shaw, and B. L. Holian, J. Chem. Phys. **80**, 1279 (1980).

[25]K. Syassen and M. Nicol, in *Physics of Solids Under High Pressures,* edited by J. S. Schilling and R. N. Shelton (North-Holland, Amsterdam, 1981), p. 33.

[26]M. L. Klein and J.-J. Weis, J. Chem. Phys. **67**, 217 (1977).

[27]M. L. Klein, D. Levesque, and J.-J. Weis, Phys. Rev. B **21**, 5785 (1980).